

Novel protein carrier system based on cyanobacterial nano-sized extracellular vesicles for application in fish

Jorge Matinha-Cardoso,^{1,2}  Filipe Coutinho,³ 
Steeve Lima,^{1,2,4}  Ana Eufrásio,^{1,2,4} 
António Paulo Carvalho,^{3,5}  Aires Oliva-Teles,^{3,5} 
José Bessa,^{1,2}  Paula Tamagnini,^{1,2,5} 
Cláudia R. Serra^{3,5,**}  and Paulo Oliveira^{1,2,5,*} 

¹IS – Instituto de Investigação e Inovação em Saúde, Universidade do Porto, Rua Alfredo Allen, 208, Porto, 4200-135, Portugal.

²IBMC – Instituto de Biologia Molecular e Celular, Universidade do Porto, Rua Alfredo Allen, 208, Porto, 4200-135, Portugal.

³CIMAR/CIIMAR – Centro Interdisciplinar de Investigação Marinha e Ambiental, Terminal de Cruzeiros do Porto de Leixões, Universidade do Porto, Av. General Norton de Matos s/n, Matosinhos, 4450-208, Portugal.

⁴MCbiology Doctoral Program, ICBAS – Instituto de Ciências Biomédicas Abel Salazar, Universidade do Porto, Rua Jorge de Viterbo Ferreira, 228, Porto, 4050-313, Portugal.

⁵Departamento de Biologia, Faculdade de Ciências, Universidade do Porto, Rua do Campo Alegre s/n, Porto, 4169-007, Portugal.

Summary

Aquaculture has been one of the fastest-growing food industry sectors, expanding at the pace of consumers' demands. To promote safe and effective fish growth performance strategies, and to stimulate environmentally friendly solutions to protect fish against disease outbreaks, new approaches are needed to safeguard fish welfare, as well as farmers and consumers interests. Here, we tested the use of cyanobacterial extracellular vesicles (EVs) as a novel nanocarrier system of heterologous proteins for applications in fish. We started by incubating

zebrafish larvae with *Synechocystis* sp. PCC6803 EVs, isolated from selected mutant strains with different cell envelope characteristics. Results show that *Synechocystis* EVs are biocompatible with fish larvae, regardless of their structural composition, as EVs neither induced fish mortality nor triggered significant inflammatory responses. We establish also that cyanobacteria are amenable to engineering heterologous protein expression and loading into EVs, for which we used the reporter sfGFP. Moreover, upon immersion treatment, we successfully demonstrate that sfGFP-loaded *Synechocystis* EVs accumulate in the gastrointestinal tract of zebrafish larvae. This work opens the possibility of using cyanobacterial EVs as a novel biotechnological tool in fish, with prospective applications in carrying proteins/enzymes, for example for modulating their nutritional status or stimulating specific adaptive immune responses.

Introduction

With an ever increasing demand for seafood that cannot be met by capture fisheries alone, growing pressure is being placed on aquaculture. According to the Food and Agriculture Organization of the United Nations, aquaculture is probably the fastest growing food-producing sector, now accounting for up to 50% of the world's fish that is used for food (FAO, 2020). However, several constraints limit the expansion of the sector, including fish growth performance in fish farms, disease outbreaks and stressful rearing conditions. Therefore, different strategies are required to maximize the welfare and nutritional status of the fish while minimizing environmental impact and feeding costs, reducing chemicals as prophylactic agents, and decreasing mortalities due to opportunistic pathogens. The use of live microorganisms as probiotics is one of such approaches (Hai, 2015), which has become popular in recent years as it reportedly improves feed value, contributes to enzymatic digestion of nutrients, inhibits the action of pathogenic microorganisms, shows anti-mutagenic and anti-carcinogenic activity, and potentiates immune responses (Pandiyani *et al.*, 2013). With the development of biotechnology, new systems and techniques have been implemented for the expression of heterologous proteins and enzymes in probiotic cells (Yao *et al.*, 2020), further potentiating their use.

Received 13 December, 2021; revised 16 March, 2022; accepted 24 March, 2022.

For correspondence. *E-mail paulo.oliveira@ibmc.up.pt; Tel. +351 226 074 900. **E-mail cserra@ciimar.up.pt; Tel. +351 220 402 777.

Microbial Biotechnology (2022) 15(8), 2191–2207

doi:10.1111/1751-7915.14057

Funding information

Fundação para a Ciência e a Tecnologia (Grant / Award Number: 'CEECIND/03482/2018', 'IF/00256/2015', 'PTDC/BIA-MOL/3834/2021', 'PTDC/BIA-OUT/29540/2017', 'SFRH/BD/130478/2017', 'SFRH/BD/147762/2019').

© 2022 The Authors. *Microbial Biotechnology* published by Society for Applied Microbiology and John Wiley & Sons Ltd.

This is an open access article under the terms of the Creative Commons Attribution-NonCommercial-NoDerivs License, which permits use and distribution in any medium, provided the original work is properly cited, the use is non-commercial and no modifications or adaptations are made.

This approach is gaining considerable interest, as these proteins and enzymes can be carefully selected to meet a specific purpose, for example increasing adherence capability, trigger adaptive immune responses or stimulate nutrient digestion (Yao *et al.*, 2020). One example is the use of microbial photosynthetic systems towards a more sustainable development of the aquaculture sector, particularly by the use of microalgae or cyanobacteria as feed or dietary supplements (Abed *et al.*, 2009; Han *et al.*, 2019; Ma *et al.*, 2020; Morais Junior *et al.*, 2020). Recently, through genetic modifications, microalgae have been engineered to express potential antigens for the development of an oral vaccination platform in fish (Kwon *et al.*, 2019). Nevertheless, the choice of whole microorganisms to use in aquaculture remains far from consensual, mainly because the gastrointestinal microbiota of aquatic organisms has been poorly characterized and the effects of the probiotics agents remain to be extensively analysed (Pandiyan *et al.*, 2013). Thus, while the realization of probiotics as protein carrier and molecular display systems is yet to be fulfilled, other alternatives are being investigated.

In the context of carrying and delivering agents with a biological effect (bioactives) (Dezfooli *et al.*, 2019), the use of bacterial extracellular vesicles (EVs) occupies a relevant position. EVs are discrete and non-replicable proteoliposomal nanoparticles (Caruana and Walper, 2020), with a size between 20 and 500 nm in diameter (Zavan *et al.*, 2020). These are bilayered nanostructures, derived from the bacterial cell envelope, containing membrane components as well as soluble products (Lima *et al.*, 2020). Gram-negative bacteria, in particular, have been extensively engineered to release EVs with customized cargo, aiming at fulfilling different purposes, namely for the delivery of chemotherapeutic agents (Kuerban *et al.*, 2020), for carrying immunogenic antigens (Fantappiè *et al.*, 2014) and even for performing complex chemical reactions extracellularly otherwise difficult to implement in whole cells (Park *et al.*, 2014). Some key features of the vesicles have encouraged these applications, particularly the fact that cargo properties are maintained in EVs even under harsh conditions, and the capacity of EVs in protecting and trafficking cargo to inaccessible targets (Bonnington and Kuehn, 2014). Despite the progress in employing EVs in biotechnology, administration to higher animals of EVs isolated from Gram-negative bacteria is usually associated with pathological reactions, including systemic inflammatory responses (Park *et al.*, 2010), mainly due to the presence of lipopolysaccharides (LPS). This represents a serious limitation, which has prompted the search for alternatives to minimize the immunogenicity of bacterial EVs, such as: the use of chemical processes to decrease LPS content, the genetic engineering of EVs-

producing bacterial strains for reduced and/or altered LPS content and the choice of bacterial strains containing LPS with low immunogenicity (Jain and Pillai, 2017). Regarding the latter, cyanobacterial derived EVs may represent a good candidate, since there are indications that cyanobacterial LPS are associated with significantly reduced toxicity in mammals, related to low immune reactivity, as compared to LPS from other bacteria (Stewart *et al.*, 2006; Durai *et al.*, 2015; Swanson-Mungerson *et al.*, 2017). Cyanobacteria are a remarkably diverse group of Gram-negative bacteria, with wide ecological distribution, and great metabolic plasticity. They are unique for being the only prokaryotes capable of performing oxygenic photosynthesis, and so, have minimal nutritional requirements. Thus, together with a wide range of genetic engineering tools available, cyanobacteria are increasingly regarded as promising, environmentally friendly and highly sustainable microbial cell factories for the production of added value products (Heidorn *et al.*, 2011). Nevertheless, the study of cyanobacterial EVs is just emerging, and many questions remain unanswered as to their potential in biotechnological applications.

The main goal of this study was, therefore, to understand to what extent are cyanobacterial EVs a viable vehicle for carrying proteins to fish. To that end, the unicellular, freshwater cyanobacterium *Synechocystis* sp. PCC6803 (hereafter *Synechocystis*) was used in this work. Different aspects had to be comprehensively analysed, including determination of toxicity of *Synechocystis* EVs and their LPS in fish, modulation of protein cargo of *Synechocystis* EVs, by packaging them with a reporter protein and evaluation of the reporter protein delivery in fish via *Synechocystis* EVs. Altogether, our results indicate that *Synechocystis* EVs represent an innovative, biocompatible protein carrier system for fish, expanding the molecular toolbox available for the transport of biologically active proteins and enzymes in aquaculture.

Results

Synechocystis wild type and mutant strains release EVs with different surface properties

Extracellular vesicles in cyanobacteria originate mainly from its cell envelope (Lima *et al.*, 2020) (Fig. 1A). In *Synechocystis*, the outermost components of the cell envelope are the S-layer and lipopolysaccharides (LPS) (Fig. 1B), which are also structural components of *Synechocystis* EVs (Fig. 1C). In this work, to evaluate the level of toxicity induced by cyanobacterial-derived EVs in fish, we started by investigating the effect of EVs isolated from *Synechocystis* on the survival and inflammatory response of zebrafish larvae. To get a deeper

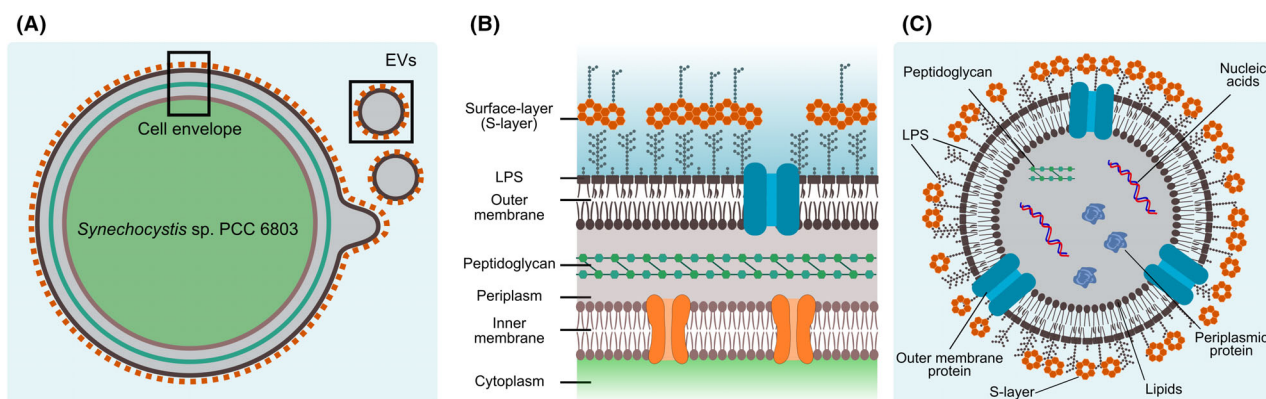


Fig. 1. Schematic representation of the structure and composition of the *Synechocystis* sp. PCC6803 cell wall and extracellular vesicles. A. Diagram showing the Gram-negative-type cell wall structure of the *Synechocystis* cell, and EVs formation by budding and detachment of the outer membrane. Squares represent close ups shown in sections B and C. B. Details of the cyanobacterial cell wall. It is worth highlighting that lipopolysaccharides constitute the outer leaflet of the outer membrane, and that the S-layer is the outermost structure of the *Synechocystis* cell. C. General view of the composition of cyanobacterial EVs.

understanding of the toxic effect of *Synechocystis* EVs components in fish, it became important to use EVs with different surface properties. To that end, different *Synechocystis* mutant strains were selected for their previously reported altered cell envelope characteristics. On one hand, the role of the S-layer was assessed by using the *tolC* mutant, which has been shown to be impaired in the secretion of the S-layer protein (protein Sll1951) (Oliveira *et al.*, 2016) as opposed to the wild-type strain (GT-Kazusa strain) that is known to produce it. On the other hand, the *fucS* mutant was selected for its unique LPS structural characteristics, as it was previously described to produce LPS with truncated *O*-antigen portions (Fisher *et al.*, 2013). Furthermore, the *tolC* mutant was reported to release more EVs than the wild-type strain (Oliveira *et al.*, 2016), which represented a trait of particular interest for subsequent assays. Another *Synechocystis* mutant strain (*tolC-spy* double mutant, Fig. S1) available in the laboratory showed slightly higher vesiculation capacity than the hypervesiculating *tolC* mutant. Thus, taking advantage of its natural capacity to produce large amounts of EVs, we decided to include the *tolC/spy* double mutant in this study as well.

Lipopolysaccharides from the *Synechocystis* wild type, and mutant strains *tolC*, *tolC/spy* and *fucS* were isolated from cells with a standard hot phenol-water method (Rezania *et al.*, 2011), and EVs were isolated by ultrafiltration and ultracentrifugation of the extracellular medium recovered from cultures of the same strains (Figs 2 and 3). After separation of the isolated samples by electrophoresis on SDS-polyacrylamide gels and subsequent detection with a LPS specific stain, it was possible to observe and confirm that the LPS band profile of the wild-type strain was similar to that of the *tolC* and *tolC-*

spy mutants, while the LPS band pattern of the *fucS* mutant strain was significantly different (Fig. 2 and Fig. S2). LPS from the *fucS* mutant show an accumulation of smooth-type LPS (lipid A, oligosaccharide core and *O*-antigen) with lower molecular weight than those of the wild-type. Comparing the LPS band profile of isolated LPS and LPS derived from EVs, one could detect a clear absence of low molecular weight, non-polar, rough-type LPS (composed of lipid A and oligosaccharide core) in the samples corresponding to isolated LPS (Fig. 2), likely resulting from the chemical-based LPS extraction protocol (Rezania *et al.*, 2011), which preferentially isolates polar molecules. Furthermore, a substantial difference could also be observed in LPS bands when comparing the various cyanobacterial samples with the commercially available LPS from *Pseudomonas aeruginosa*, used here as reference.

Isolated EVs were also characterized in detail in terms of their abundance, morphological aspect and size (Fig. 3). Determination of the amount of EVs produced by each strain, indicated that *tolC*, *tolC-spy* and *fucS* are hypervesiculating strains (Fig. 3A). This relative EVs production capacity could already be observed during the EVs isolation protocol: after the ultracentrifugation step, EVs pellets from all *Synechocystis* strains showed the typical orange pigmentation, consistent with the presence of carotenoids in the outer membrane of this cyanobacterium, with vesicles from the wild-type corresponding to the smallest pellet (Fig. 3B). Despite the differences in abundance, isolated EVs from the various cyanobacterial strains appeared as spherical nanosized structures when observed by transmission electron microscopy (TEM) of negatively stained samples (Fig. 3B). Based on these transmission electron

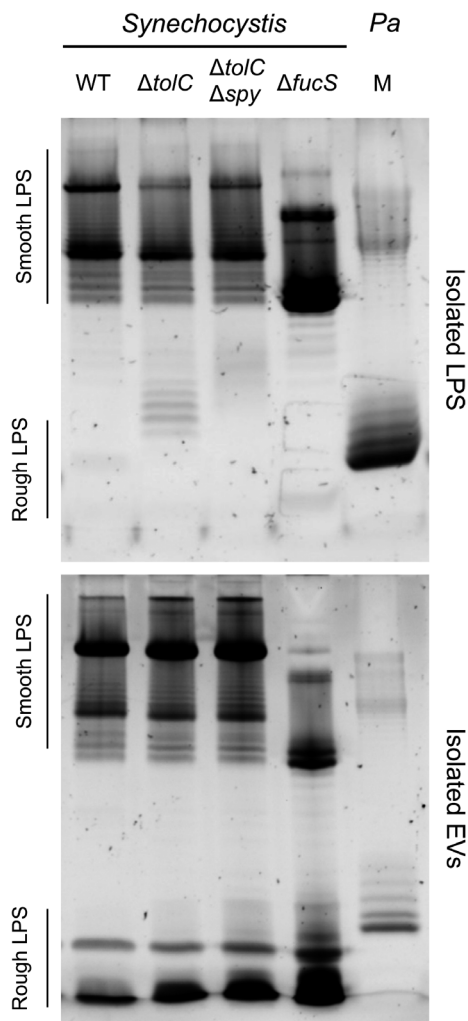


Fig. 2. Lipopolysaccharides (LPS) band profile of isolated LPS and of purified extracellular vesicles obtained from the *Synechocystis* sp. PCC6803 strains studied in this work. LPS from the *Synechocystis* wild-type (WT), and mutant strains $\Delta tolC$, $\Delta tolC/\Delta spy$ and $\Delta fucS$ were isolated with a standard hot phenol-water method (Rezania *et al.*, 2011) (upper panel), while EVs from the same strains were collected from the spent medium by ultrafiltration and ultracentrifugation (bottom panel). LPS present in both sample types were separated on 16% (w/v) SDS-polyacrylamide gels, and stained with the Pro-Q™ Emerald 300 Lipopolysaccharide Gel Stain Kit (Life Technologies). Commercial LPS from *Pseudomonas aeruginosa* (LPS Pa) was loaded as reference marker (M). High molecular LPS (containing lipid A, oligosaccharide core and O-antigen) are shown as Smooth LPS, and low molecular LPS (containing lipid A, oligosaccharide core) are indicated as Rough LPS. These gels are representative of the results obtained from at least three independent biological replicates.

micrographs, the size of isolated EVs was determined. While EVs from the wild-type and *fucS* mutant strain are more heterogeneous in size distribution, those isolated from the *tolC* and *tolC-spy* mutant strains are enriched in a narrower size range. Approximately 50% of the measured EVs were found to have a diameter between 45

and 60 nm in the *tolC* and *tolC-spy* mutant strains, and between 45 and 70 nm, and 35 and 60 nm for the wild-type and *fucS* mutant respectively (Fig. 3B). Moreover, abnormally large EVs (larger than 130 nm in diameter) could also be observed in the *fucS* mutant strain, which corresponded to more than 10% of all the measured EVs.

Isolated Synechocystis LPS and EVs do not induce zebrafish larvae mortality

We then proceeded to evaluate the biocompatibility of isolated *Synechocystis* LPS and EVs in fish. Three days post-fertilization (dpf) zebrafish (*Danio rerio*) larvae were treated by immersion with different amounts of cyanobacterial LPS or EVs for 5 days, and zebrafish larval survival was monitored daily. In addition, commercially available LPS from *P. aeruginosa* were also included in the test, as these have been reported to induce approximately 50% larval mortality in about 8 h of treatment with $50 \mu\text{g ml}^{-1}$ (Novoa *et al.*, 2009). Altogether, our results showed that neither EVs from any of the cyanobacterial strains used in this work nor isolated cyanobacterial LPS from the wild-type or the *tolC* and *fucS* single mutants induced significant mortality in zebrafish larvae under the tested conditions (Fig. 4; Tables S1 and S2–S5). In contrast, larvae exposed to $500 \mu\text{g ml}^{-1}$ of LPS isolated from the cyanobacterial *tolC-spy*-double mutant, and to a lesser extent $250 \mu\text{g ml}^{-1}$ of LPS, showed a significant reduction in survival rate, although not as severe as that obtained with the *P. aeruginosa* LPS. Thus, while $45 \mu\text{g ml}^{-1}$ *P. aeruginosa* LPS triggered > 80% mortality after 24 h of treatment, isolated EVs concentrations of up to $500 \mu\text{g ml}^{-1}$ from *Synechocystis* may be used without significantly reducing larvae survival.

EVs from the Synechocystis tolC and fucS mutant strains do not trigger high inflammation responses

Taking advantage of the hypervesiculating phenotype of *tolC* and *fucS* single mutants, the innate immune response of zebrafish larvae to EVs isolated from these mutants was evaluated in 3 dpf zebrafish larvae subject to a 24 h immersion trial, against a zebrafish embryo medium control treatment (the *tolC-spy* mutant was not included, as its LPS showed some level of toxicity). The expression of pro-inflammatory cytokine interleukin 1 beta (IL-1 β), tumour necrosis factor (TNF- α) and anti-inflammatory cytokine interleukin 10 (IL-10), was then analysed by RT-qPCR and results normalized by RPL13a mRNA levels (Fig. 5 and Table S6). In contrast to LPS from *P. aeruginosa* that induced significant upregulation of inflammatory markers, when used at a sub-lethal concentration of $35 \mu\text{g ml}^{-1}$, EVs isolated from the

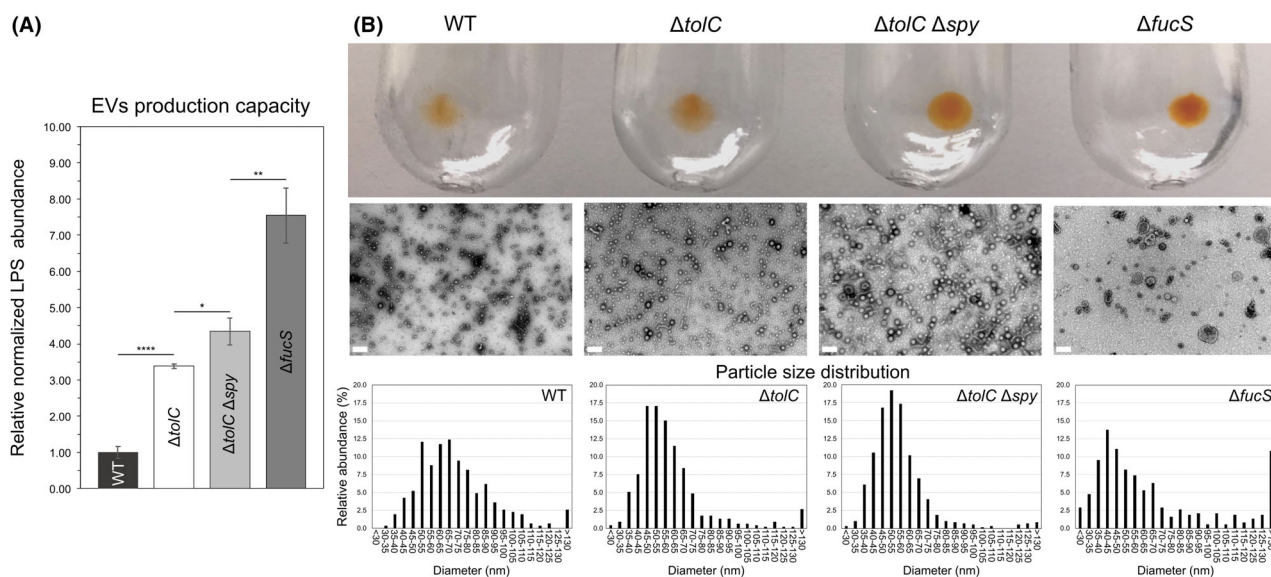


Fig. 3. Characterization of the *Synechocystis* sp. PCC6803 extracellular vesicles isolated from the wild-type and mutant strains. A. Relative vesicle production capacity of *Synechocystis* wild type (WT), and *tolC* ($\Delta tolC$), *tolC/spy* ($\Delta tolC/\Delta spy$) and *fucS* ($\Delta fucS$) mutant strains, as determined by densitometry analysis of the outer membrane marker LPS detected on SDS-polyacrylamide gels (Fig. S2). For LPS quantitation, images of stained gels were processed using ImageJ by quantifying pixel intensity values of all bands detected in a given lane, and deducing LPS amount against a calibration curve established with *P. aeruginosa* LPS (Sigma-Aldrich, Burlington, MA, USA) as standard. EVs samples were normalized to culture OD₇₃₀, culture volume, and final EVs sample volume, prior to separation by electrophoresis. Error bars indicate standard deviations of three independent biological replicates. Statistical analysis was performed by means of a one-way ANOVA. *, $P < 0.05$; **, $P < 0.01$; ****, $P < 0.0001$.

B. Pellets resulting from the ultracentrifugation step during EVs isolation from the *Synechocystis* wild-type and mutant strains are shown (top panels). Transmission electron micrographs of negatively stained isolated EVs samples of the various *Synechocystis* strains show details of their size and morphology (middle panels) (scale bar: 200 nm). Note that the relative amount of EVs isolated from each strain cannot be assessed in these micrographs, as different amounts of EVs were loaded onto the grids for optimized visualization. Histograms showing particle size distribution of EVs samples from the different cyanobacterial strains are presented (bottom panels). EVs were separated in 5 nm size groups, distributed between 30 and 130 nm, and in groups comprising those with a size below 30 nm or higher than 130 nm. Vesicle diameter was determined by direct measurement from electron micrographs of three independent biological replicates. Abundance of each size group is presented as relative figures, that is number of vesicles with a given diameter range relative to the total number of vesicles measured. More than 300 vesicles were measured for the wild-type, 450 for the *tolC* mutant, 550 for the double *tolC-spy* mutant, and 350 for the *fucS* mutant.

tolC and *fucS* single mutants were shown not to induce a significant inflammatory response even at a concentration of $500 \mu\text{g ml}^{-1}$. The observation that *Synechocystis* EVs harbouring LPS with different O-antigen length and characteristics do not trigger acute inflammation in fish, further supports that *Synechocystis* EVs structural components are biocompatible with fish even at high concentrations.

Modulation of *Synechocystis* EVs protein content

To evaluate the capacity of customizing the protein content of *Synechocystis* EVs, the super-folder green fluorescent protein (sfGFP) was used as reporter, as recently described (Lima *et al.*, 2022). Hence, sfGFP was expressed in *Synechocystis* cells under the control of the well-characterized, strong promoter $P_{trc.x.lacO}$ (Ferreira *et al.*, 2018) and further targeted to the periplasm by the signal peptide of the *Synechocystis* periplasmic protein FutA2, a substrate of the twin-arginine translocation (Tat) pathway (Waldron *et al.*, 2007; Badarau *et al.*,

2008) (Fig. 6). Plasmids pEV-trc-GFP(S) were constructed for this purpose, and despite various transformation attempts in the hypervesiculating *Synechocystis* *tolC* mutant strain, sfGFP expressing cyanobacteria were only possible to obtain with wild-type cells as background strain. Fully segregated cells (EV-trc-GFP) were cultivated in liquid medium, and a yellowish/greenish coloration of the extracellular medium could be observed (Fig. 6A). Cells were studied by confocal microscopy to evaluate sfGFP expression and cellular localization of the fluorescent signal (Fig. 6B). The sfGFP-dependent fluorescent signal was localized outside of the autofluorescence signal, which derives from the photosynthetic pigments located in the thylakoid membranes, indicating that most of the sfGFP protein is in the periplasm of cyanobacterial cells (Fig. 6C). Occasionally, it was also possible to observe small fluorescent foci in the extracellular medium. Thus, the extracellular medium of EV-trc-GFP cells was collected, and the respective EVs were isolated. The EV-free extracellular medium was also further concentrated and analysed. Western blotting analysis of

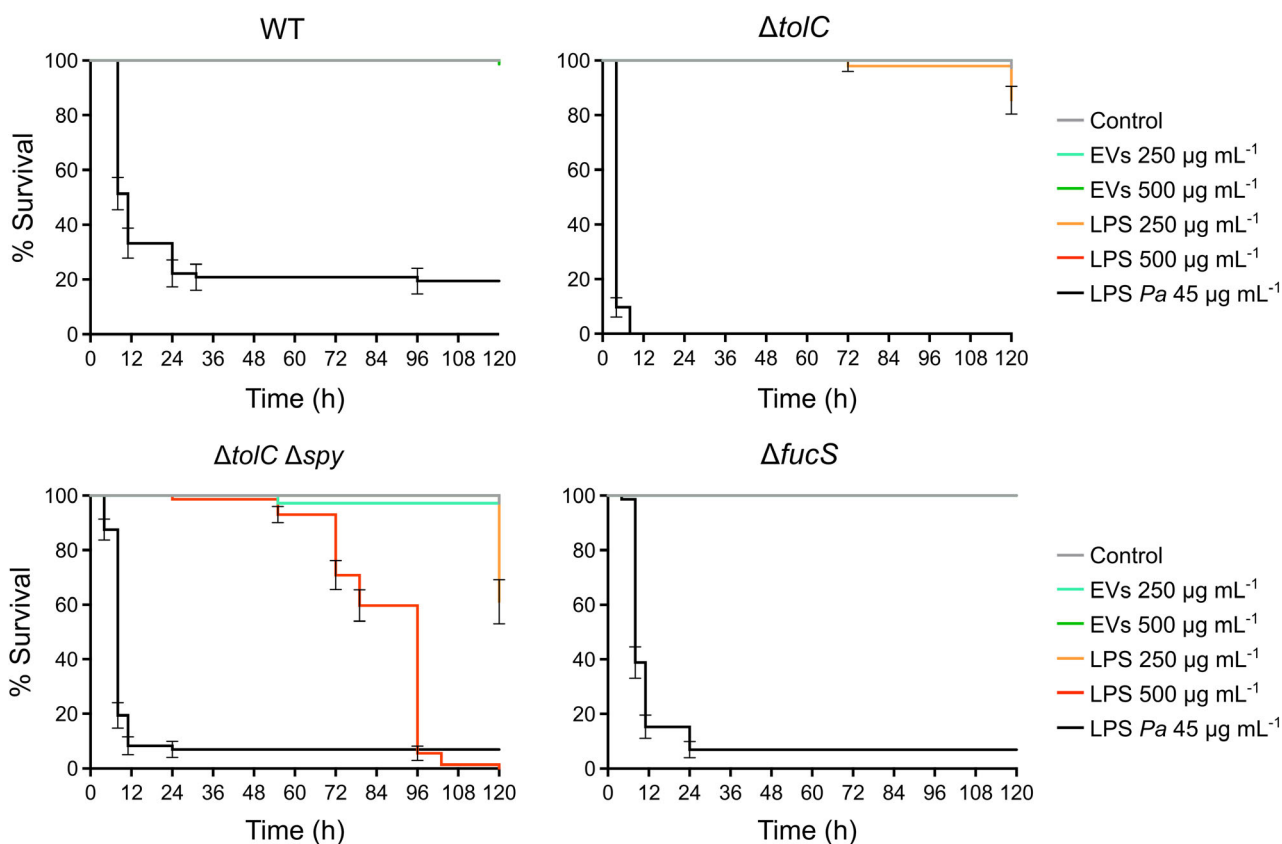


Fig. 4. Effect of isolated lipopolysaccharides and extracellular vesicles from the *Synechocystis* sp. PCC6803 strains studied in this work on zebrafish larvae survival. Kaplan–Meier survival curves of 3 days post-fertilization (dpf) zebrafish larvae subjected to zebrafish embryo medium containing 250 or 500 $\mu\text{g mL}^{-1}$ of isolated LPS or EVs from *Synechocystis* sp. PCC6803 wild-type (WT), and mutant strains ΔtolC , $\Delta\text{tolC}/\Delta\text{spy}$ and ΔfucS . Survival tests also included two control treatments, which were carried out separately for each set of experiments corresponding to each *Synechocystis* strain. Control treatments received either zebrafish embryo medium only (Control) or zebrafish embryo medium containing commercial LPS from *Pseudomonas aeruginosa* (LPS *Pa*) at 45 $\mu\text{g mL}^{-1}$. Survival was monitored for 5 days (120 h) of immersion challenge. Data are represented as mean \pm standard deviation of two independent biological experiments, each condition tested in triplicates of 12 larvae, making a total of 72 larvae analysed within each experimental condition. Survival percentages data points are listed in Table S1.

the various fractions, using a GFP-specific antibody, determined that EV-trc-GFP cells indeed express sfGFP, in agreement with confocal microscopy results and that the reporter successfully accumulates in the extracellular medium, both in isolated EVs fractions and in concentrated EV-free extracellular medium (Fig. 6D). Moreover, it was possible to quantify that approximately 90% of the sfGFP protein present in the extracellular medium was found soluble in the medium, with the remaining part present in the isolated EVs fraction (Fig. 6D).

Characterization of EVs obtained from the EV-trc-GFP strain was carried out by different microscopic methods. Confocal microscopy observations of isolated EVs preparations determined the existence of numerous, highly fluorescent foci in the sample (Fig. 6E), consistent with possible sfGFP-packed EVs. TEM analysis of negatively stained samples indicated the presence of many spherical nanostructures, morphologically similar to EVs from the *Synechocystis* wild-type and mutant strains studied in this work (Fig. S3A). Moreover, TEM analysis of

immunogold labelled EVs samples demonstrated the presence of sfGFP inside EVs (Fig. 6E). To complement the characterization of sfGFP-packed EVs, isolated samples were investigated by LPS analysis upon electrophoretic separation on SDS-polyacrylamide gels, and by determining their size from the analysis of TEM micrographs (Fig. S3B and C). The results indicate that strain EV-trc-GFP releases approximately 3.5-fold more EVs than the wild-type strain, and that sfGFP-containing EVs are slightly smaller than EVs from any other strain investigated in this study (50% of the analysed EVs had a diameter between 35 and 55 nm).

sfGFP-loaded Synechocystis EVs reach the gastrointestinal tract of zebrafish larvae upon immersion treatment

To understand whether cyanobacterial EVs can work as nanocarriers of custom proteins into fish, 5 dpf zebrafish larvae were treated by immersion with isolated sfGFP-

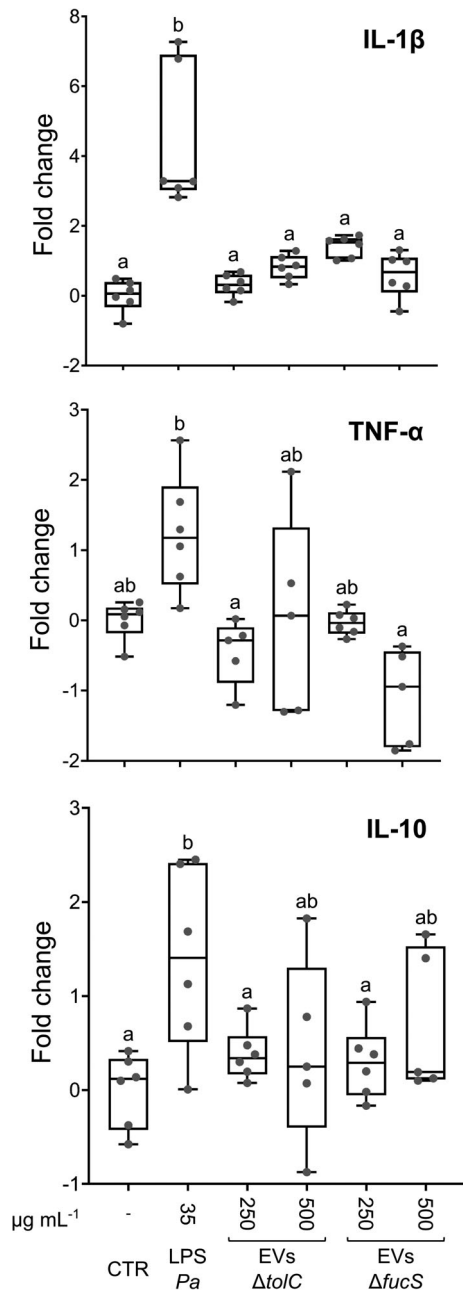


Fig. 5. Effect of isolated extracellular vesicles from the *Synechocystis* sp. PCC6803 mutant strains $\Delta tolC$ and $\Delta fucS$ on the expression of fish inflammation markers. Quantitative expression analysed by RT-qPCR of the genes encoding Interleukin 1 beta (IL-1 β), Tumor necrosis factor alpha (TNF- α), and Interleukin 10 (IL-10) in zebrafish larvae immersed in zebrafish embryo medium only (CTR – control), zebrafish embryo medium containing 250 or 500 $\mu\text{g mL}^{-1}$ of EVs from *Synechocystis* mutants $\Delta tolC$ (EVs $\Delta tolC$) and $\Delta fucS$ (EVs $\Delta fucS$), or in zebrafish embryo medium containing 35 $\mu\text{g mL}^{-1}$ of *P. aeruginosa* (LPS *Pa*). For each treatment, 6 pools of 20 larvae each were analysed (individual data points are shown). Extreme outliers (for details, see Experimental procedures) were removed from the analysis. Treatments effects were analysed by one-way ANOVA and significant differences among means ($P < 0.05$) were determined by the Tukey's multiple range test (for details, see Table S6).

loaded *Synechocystis* EVs for 24 h. In agreement with earlier observations (Fig. 4), zebrafish larvae treated with EVs did not show signs of morbidity, and did not die. Upon treatment, larvae were euthanized and observed by confocal microscopy. Under the microscope, while a clear fluorescence signal could be observed in the ventral region of zebrafish larvae treated with sfGFP-loaded EVs, control larvae (in which no EVs were added) did not show fluorescence signal (Fig. 7). Closer inspection of the signal in respect to the zebrafish larvae anatomy indicated that it originates mainly from the gastrointestinal (GI) tract of the animal, particularly the intestine. This observation establishes that *Synechocystis* EVs with customized protein cargo: (i) can be suspended in the medium where zebrafish larvae are maintained; (ii) are ingested by the animals; (iii) accumulate in the GI tract; and (iv) can help to maintain structure and activity of the heterologous protein, as sfGFP retained its fluorescence throughout the whole process.

Discussion

One of the main objectives of this work was to determine to what extent are cyanobacterial-derived EVs toxic to fish. To meet that goal, we decided to use the well-characterized unicellular cyanobacterium *Synechocystis*, and zebrafish (*Danio rerio*) as model organisms. On one hand, as EVs are nanostructures that result from the release of material from the bacterial cell envelope (Figs 1–3), we decided to include various *Synechocystis* mutant strains with different cell envelope/surface properties, and differential vesiculation capacity. On the other hand, analysis of immune responses in zebrafish are simplified with the use of individuals in their larval stage, as they are transparent, easy to cultivate and only the innate immune system is present, allowing the assessment of physiological responses with the whole organism (Novoa *et al.*, 2009).

Immersion trials using 3 dpf zebrafish larvae and isolated LPS or EVs from the various genetically engineered *Synechocystis* strains did not show severe mortality as compared to the control condition (*P. aeruginosa* LPS (Novoa *et al.*, 2009)), except for LPS isolated from the *tolC-spy* mutant strain (Fig. 4). In previous work, we have found that absence of a functional TolC protein in *Synechocystis* results in high intracellular oxidative stress, as indicated by the accumulation of reactive oxygen species (ROS) in the cytoplasm and high level of lipid peroxidation (Hewelt-Belka *et al.*, 2020), with the consequent activation of ROS detoxifying enzymes (Oliveira *et al.*, 2016). Moreover, we have also found that cell envelope stress pathways are upregulated in the *tolC* mutant, as indicated by upregulation of transcript levels of genes (*spy*, *degQ*) and

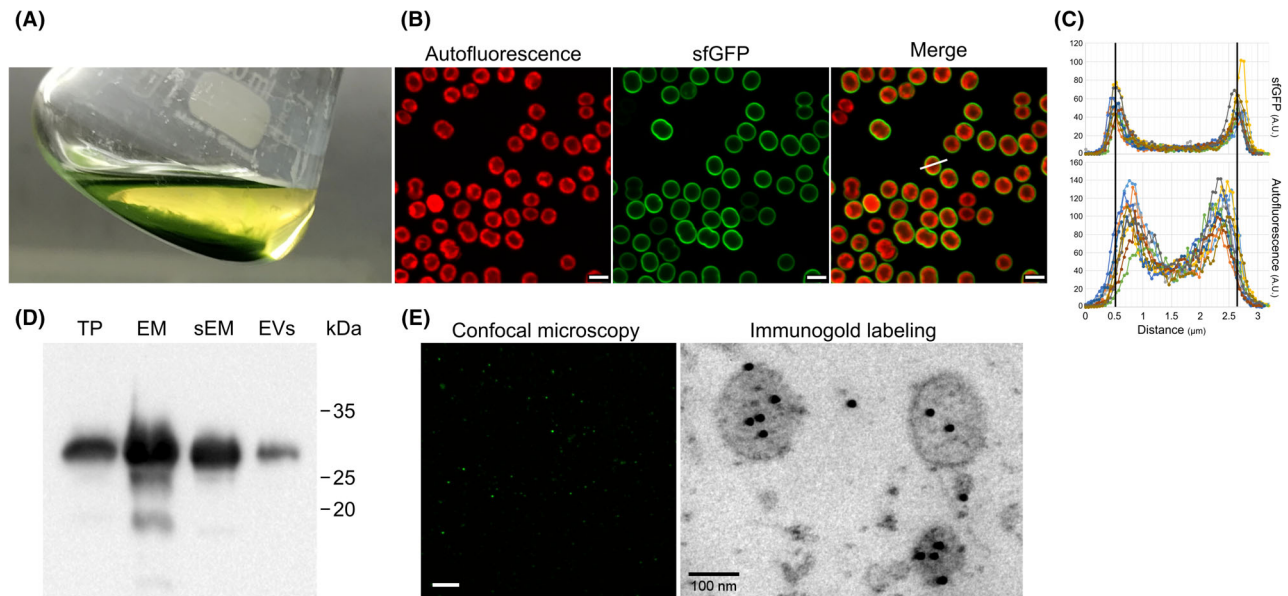


Fig. 6. *Synechocystis* sp. PCC6803 extracellular vesicles loaded with the reporter sfGFP.

A. Photograph of a liquid culture of EV-trc-GFP (*Synechocystis* cells expressing sfGFP fused with the signal peptide of the FutA2 protein, under the control of the $P_{trc.x.lacO}$ promoter), showing details of the yellow/green colour found in the extracellular medium.

B. Confocal micrographs of EV-trc-GFP cells depicting the red autofluorescence signal from the photosynthetic pigments (Autofluorescence), and the green signal from the sfGFP reporter (sfGFP). A panel showing the result of merging the two micrographs is also presented (Merge). Scale bar: 3 μ m.

C. sfGFP (upper panel) and autofluorescence (bottom panel) fluorescence intensity plots determined for 10 different EV-trc-GFP cells (a.u., arbitrary units). Fluorescence intensity was quantified across the chosen cells as indicated by the white line drawn over one of the EV-trc-GFP cells in the merged fluorescence signal confocal micrograph, and plotted against line distance (in μ m).

D. Western blot analysis for the detection of sfGFP protein in 10 μ g of total cellular protein (TP), and cell free concentrated extracellular media (EM) samples of EV-trc-GFP cells. From the whole extracellular medium sample, extracellular vesicles (EVs) were separated from the soluble part (sEM), and also included for analysis. EM, sEM and EVs samples were normalized for initial cell-free culture volume concentrated, final volume of concentrated sample, and culture OD_{730} . This blot is representative of the results obtained from three independent biological replicates.

E. Microscopic analyses of EVs isolated from EV-trc-GFP cells, including a confocal micrograph showing green fluorescent foci (scale bar: 5 μ m), and a transmission electron micrograph of immunogold labelled EVs. Black dots indicate the presence of sfGFP epitopes.

overexpression of proteins (Spy, DegP) (Gonçalves *et al.*, 2018) related to envelope stress responses. These results highlight that the *tolC* mutant is under stress, with undergoing adaptations at the periplasmic level. Spy is an important periplasmic chaperone, contributing to protein folding in the periplasm (Quan *et al.*, 2011). Deletion of *spy* in the *tolC* mutant background resulted in higher vesiculation (Fig. 3), which could be interpreted as a sign of further stress. Thus, it is possible that *tolC-spy* double mutant cells are under higher oxidative stress than *tolC* cells, which could lead to an increased level of LPS oxidation. Consequently, we hypothesize that LPS from the *tolC-spy* mutant are more toxic than LPS isolated from other *Synechocystis* strains used in this work, which could account for the differences observed in the zebrafish survival tests. However, despite the higher toxicity of its LPS, EVs isolated from *tolC-spy* mutant did not induce significant mortality in zebrafish larvae. This may be related to the bioavailability of isolated LPS versus LPS in vesicles to fish cells and tissues under the tested conditions. Still, the mortality observed with the

LPS isolated from the double mutant strain seems to confirm that LPS are the most immunogenic structural components of EVs.

Expression analysis of molecular markers associated with inflammatory responses in fish, namely IL-1 β , TNF- α and IL-10, showed their significant upregulation in zebrafish larvae exposed to sub-lethal concentrations of *P. aeruginosa* LPS, but not to isolated *Synechocystis* EVs of the *tolC* and *fucS* mutant strains, even when high amounts of EVs were used (Fig. 5). Altogether, these results indicate that zebrafish larvae can withstand high dosages of *Synechocystis* LPS and EVs, without triggering systemic inflammatory responses. This is in agreement with earlier works reporting a significantly reduced toxicity of LPS isolated from various cyanobacterial strains (*Anacystis nidulans*, *Oscillatoria* sp. and species of the genera *Anabaena*, *Aphanizomenon*, *Microcystis* and *Nodularia*) compared to LPS from other bacteria (*Escherichia coli*, *Salmonella* sp.) (Stewart *et al.*, 2006; Durai *et al.*, 2015; Swanson-Mungerson *et al.*, 2017). This low reactivity against cyanobacterial LPS can be

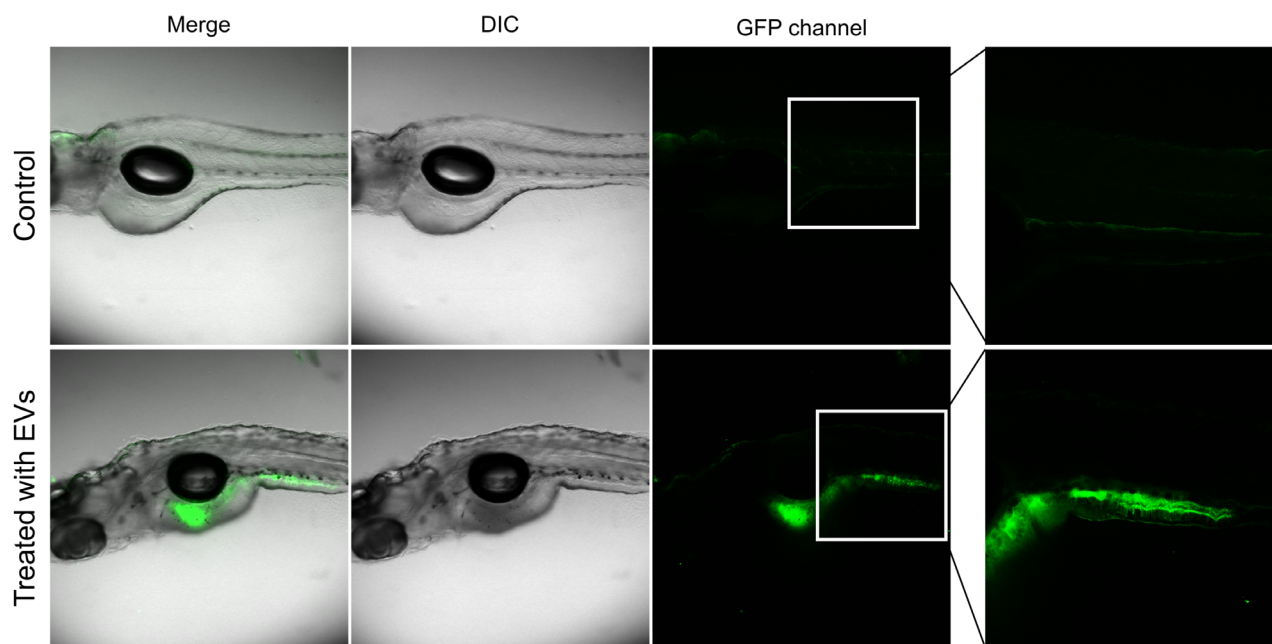


Fig. 7. *Synechocystis* extracellular vesicles loaded with sfGFP accumulate in the gastrointestinal tract of zebrafish larvae. Confocal micrographs of 5 dpf zebrafish larvae subjected for 24 h to immersion trials without (Control – upper panels) or with $1000 \mu\text{g ml}^{-1}$ sfGFP-loaded EVs isolated from the cyanobacterial strain EV-trc-GFP (lower panels). The differential interference contrast (DIC) micrographs are shown in the middle panels, while the fluorescence signal detected in the GFP channel (excitation: 488 nm; emission: 495–540 nm) are shown on the right hand panels. The result of merging the DIC and GFP channel micrographs is presented on the left-hand side (Merge). The white square in each ‘GFP channel’ micrograph indicates the position where a larger magnification of the anatomic region corresponding to the gastrointestinal tract was obtained (right-hand side).

explained by structural differences detected in the cyanobacterial lipid A backbone, as compared to other Gram-negative bacteria (Hahn and Schleiff, 2014). In particular, a missing phosphorylation at position 1-4' of the glucosamine disaccharide in the cyanobacterial lipid A has been suggested to represent the key factor associated with cyanobacterial LPS-reduced toxicity (Hahn and Schleiff, 2014). Additional biochemical and structural studies are needed to fully elucidate this effect.

In addition to showing that high amounts of *Synechocystis*-derived EVs are not toxic to zebrafish larvae, in this study we also present evidence supporting the capacity of customizing protein cargo of *Synechocystis* EVs (Fig. 6). By fusing the reporter sfGFP with the Tat-dependent signal peptide of protein FutA2 (Waldron *et al.*, 2007; Badarau *et al.*, 2008) as previously described (Polyviou *et al.*, 2018), we were able to show expression and translocation of sfGFP to the periplasm and, ultimately, to EVs. Loading of EVs with proteins of interest has long been shown for example for *E. coli* (Kesty and Kuehn, 2004), and here, we demonstrate that the protein content of *Synechocystis* EVs can also be customized with a heterologous protein. Curiously, strain EV-trc-GFP showed an increased vesiculation capacity as compared to the wild-type strain (Fig. S3). This observation is consistent with the possibility of an

increased ‘periplasmic pressure’ resulting from an accumulation of protein in the periplasm, as suggested by Schwechheimer *et al.* (2014). In fact, this pressure could also account for the difficulty in transforming the sfGFP construct into the *tolC* mutant background: as discussed above, this hypervesiculating mutant strain is under oxidative stress, with several adaptations at the periplasmic level. With this construct, protein expression is under the control of the constitutive, relatively strong promoter $P_{trc.x.lacO}$ (Ferreira *et al.*, 2018), and translocation to the periplasm seems to be rather efficient, likely recruiting several Tat transporters, as indicated by the accumulation of sfGFP signal in the periplasm as compared to that in the cytoplasm (Fig. 6C). Thus, over accumulation of protein in the periplasm may lead to an increase in periplasmic pressure, which in turn leads to hypervesiculation in the wild-type strain, but impairs growth in the *tolC* mutant. In the future, expression of sfGFP with a weak promoter in the *tolC* mutant will help in clarifying whether the strain can cope with low sfGFP abundance in the periplasm and release EVs packed with the reporter.

Several aspects require optimization towards an efficient loading of cyanobacterial EVs with proteins of interest, including fine-tuned expression of the protein, translocation to the periplasm, protein-folding and

-stability in the periplasm, and efficient targeting to EVs. Adjusting these aspects brings the prospect of making cyanobacteria sustainable microbial factories for the production of safe EVs, suitable for various biotechnological applications. In that line of thinking, cyanobacterial EVs have already been used with success to stimulate cutaneous wound healing in mice, by promoting angiogenesis (Yin *et al.*, 2019).

Here we also established that sfGFP-loaded EVs from *Synechocystis* can successfully carry the customized protein cargo to fish, as illustrated by the detection of sfGFP signal in the GI tract of zebrafish larvae upon immersion treatments. The uptake and biodistribution of nanoparticles (in the range of 25–100 nm) in zebrafish larvae have been described before, but the focus has been mainly on nanoplastics in the context of environmental pollution (van Pomeran *et al.*, 2017; Pitt *et al.*, 2018; Sendra *et al.*, 2021). Curiously, these nanoparticles could also be detected in the GI tract of the animals analysed, which further supports the notion that nano-sized EVs in suspension will follow the same internalization route towards the fish gut, naturally accumulating in the intestine. The fact that sfGFP signal is detected in a concentrated manner (Fig. 7) suggests prolonged residence time of the protein in the gut environment. However, several questions remain to be addressed: are the EVs degraded, and, if so, is the protein cargo released to the gut environment? Can the EVs be internalized integrally by gut cells? Can EVs even cross the gut-blood barrier and reach the blood stream? Previous work using unicellular microalgae expressing GFP also showed accumulation of fluorescence signal in zebrafish intestinal tissues (Kwon *et al.*, 2019). The authors hypothesized that the microalgal cell wall is broken down in the hind gut by cellulolytic commensal bacteria, and, consequently, the recombinant protein is released and absorbed by intestinal cells (Kwon *et al.*, 2019). In the case of *Synechocystis* EVs, this may also occur. However, it is also possible that these nano-sized structures are internalized by gut cells, releasing their cargo therein. In fact, several cellular entry pathways of bacterial EVs have already been described in eukaryotic hosts (O'Donoghue and Krachler, 2016). In this context, if the goal is to promote the absorption of a protein of interest, cellular uptake of EVs may be an advantage over the use of whole-cell microbes. For other biotechnological applications, however, the release of protein cargo from EVs may not even be required. If the protein is an enzyme, it could benefit its activity to be shielded inside the vesicle against proteolytic activity (Alves *et al.*, 2016). In this case, the enzyme substrate could cross the membrane of the vesicle, enabling the reaction to ensue (Biller *et al.*, 2022a). Future work should address these questions in order to explore the full potential of

Synechocystis EVs as effective carrier systems for different types of applications in fish.

In summary, this work presents an innovative protein carrier system to address several challenges in the fish production sector. Whether one envisions fine-tuning metabolic functions in fish towards an improved nutritional status, or modulating its immune system to generate specific immune responses against selected antigens, stimulating protection against a given pathogenic agent, customized cyanobacterial EVs have the prospect of becoming serious nanocarriers for the targeted delivery of specific proteins to fish. Future studies will clarify how cyanobacterial EVs can be best administered to fish (e.g. immersion, oral or injection) without compromising delivery efficacy and maximizing protein/enzyme activity.

Experimental procedures

Cyanobacterial strains and routine cultivation conditions

The cyanobacterium *Synechocystis* sp. PCC6803 wild-type (sub-strain GT-Kazusa; glucose tolerant, with S-layer and non-motile) and mutant strains *tolC* (Oliveira *et al.*, 2016), and *tolC-spy*, *fucS* and EV-trc-GFP (this work) (list of strains is available in Table S7) were maintained in liquid BG11 medium (Rippka *et al.*, 1979) in 100 ml Erlenmeyer flasks, kept on an orbital shaker (100 r.p.m.), under a 16 h light (OSRAM Lumilux, 18W/865, Cool daylight) (30–40 $\mu\text{mol photons m}^{-2} \text{s}^{-1}$)/8 h dark regimen, at 28°C. In the case of the mutant strains, medium was supplemented with antibiotics: 100 $\mu\text{g kanamycin ml}^{-1}$ for *tolC*, *fucS* and EV-trc-GFP; and 50 $\mu\text{g kanamycin ml}^{-1}$, and 2 $\mu\text{g spectinomycin ml}^{-1}$ and 2 $\mu\text{g streptomycin ml}^{-1}$ for the double mutant *tolC-spy*. Growth was monitored spectrophotometrically by analysing optical density at 730 nm (OD_{730}). Routinely, cyanobacterial strains were streaked on solid BG11 medium plates to assess the axenic state of the cultures.

Generation of Synechocystis deletion mutant strains $\Delta\text{tolC}/\Delta\text{spy}$ and ΔfucS

To generate the deletion mutant strains used in this work, the *Synechocystis* natural transformation capability and gene replacement by double homologous recombination were used as previously described (Heidorn *et al.*, 2011). Briefly, two DNA fragments of approximately 600 bp, in the vicinity of both the *spy* gene (*sl10858*) and the *fucS* gene (*sl11213*) were amplified by PCR using specific oligonucleotides (see Table S8). For both cases, the DNA fragment closer to the 5' region of the gene of interest was digested with the restriction enzymes XhoI and PstI, while the fragment closer to the 3' region of

the gene of interest was digested with PstI and BamHI. All the restriction sites were included in the sequence of the oligonucleotides (Table S8). The two DNA fragments for each gene deletion were then ligated simultaneously to the plasmid pSKII + (Stratagene), previously digested with XhoI and BamHI, rendering plasmids pSpy and pFucS, for deletion of the *spy* and *fucS* genes respectively. The identity of the fragments was determined by Sanger sequencing (StabVida). Then, DNA fragments containing the determinants for conferring antibiotic resistance, either for spectinomycin/streptomycin or for kanamycin, were amplified by PCR with specific oligonucleotides, containing the recognition site for the restriction enzyme PstI. While the spectinomycin/streptomycin resistance cassette was used to replace the nucleotide sequence of the *spy* gene between positions 127 and 549 relative to the first nucleotide of the gene, the kanamycin resistance cassette was used to replace the nucleotide sequence of the *fucS* gene between positions 131 and 678. Thus, plasmids pSpy and pFucS were linearized with PstI, and the antibiotic resistance cassettes previously digested with PstI were ligated to the respective plasmids, rendering plasmids pSpy-SpSm and pFucS-Km respectively.

Synechocystis wild type and *tolC* mutant were then cultivated up to an OD₇₃₀ of about 0.5, and naturally transformed with plasmids pFucS-Km and pSpy-SpSm, respectively, as described elsewhere (Pinto *et al.*, 2015). Fully segregated mutants were selected by increasing concentration of the respective antibiotic, and segregation was assessed by PCR using specific oligonucleotides.

Engineering of *Synechocystis* heterologous protein expression and targeting to EVs

To construct the *Synechocystis* strain expressing the heterologous protein sfGFP and further targeting it to extracellular vesicles (Lima *et al.*, 2022), the synthetic promoter P_{trc.x.lacO} (Ferreira *et al.*, 2018) the signal peptide sequence of the *Synechocystis* native protein FutA2 (amino acids 1 to 35) as previously used by Polyviou *et al.* (2018), which determines its translocation to the periplasm, and the gene encoding the reporter protein super-folder Green Fluorescent Protein (sfGFP) were amplified by PCR using specific oligonucleotides (Table S8). Assembly of the different DNA fragments was performed by sequential overlap-extension PCR. The 953 bp fragment was digested with PstI and XbaI, and ligated either to plasmid pSN15KPO or to plasmid pSN15S previously digested with the same restriction enzymes, rendering plasmids pEV-trc-GFP and pEV-trc-GFPS. Identity of the fragment in each plasmid was determined by Sanger sequencing. Plasmids pSN15KPO

and pSN15S are variants of plasmid pSN15K (Pinto *et al.*, 2015), in which the original kanamycin resistance cassette was replaced by that present in plasmid pUC4K (GE Healthcare), or by the spectinomycin/streptomycin resistance cassette from plasmid pRL278 (Cai and Wolk, 1990) respectively. *Synechocystis* wild-type cells were naturally transformed with pEV-trc-GFP, and fully segregated mutants were obtained, while *Synechocystis tolC* mutant cells were transformed with pEV-trc-GFPS, but without resulting in transformed colonies.

Isolation of *Synechocystis* lipopolysaccharides and extracellular vesicles

To isolate cyanobacterial LPS and EVs, cells from *Synechocystis* wild-type and mutant strains *tolC*, *tolC/spy*, *fucS* and EV-trc-GFP were cultivated in glass gas washing bottles with aeration (1L air min⁻¹), under a 16h light (30–40 μmol photons m⁻² s⁻¹)/8 h dark regime, at 28°C. Cultures were grown until an OD₇₃₀ of approximately 1.5. LPS were isolated by the hot phenol-water method as previously described (Rezania *et al.*, 2011), recovering LPS from the aqueous phase (LPS in the organic phase were discarded, as it was difficult to remove contaminating phenol even after several rounds of dialysis), and storing them at –20°C until further analysis. Regarding EVs' isolation, *Synechocystis* cultures were centrifuged at 4400 g for 10 min at room temperature to separate cells from the extracellular medium. A total volume of 3.6 l of extracellular medium, unless stated otherwise, was filtered through 0.45 μm pore size filters, and further concentrated by ultrafiltration using centrifugal filters with a molecular weight cut-off of 100 kDa (Millipore, Burlington, MA, USA). A final volume of approximately 15 ml of concentrated extracellular medium was then centrifuged at 100 000 g for 3 h, at 4°C, as previously described (Biller *et al.*, 2022b). The resulting EVs pellets were then suspended in sterile BG11 medium and stored at –80°C until further analysis.

For both isolated LPS and isolated EVs, the amount and band profile of LPS were routinely analysed. LPS and EVs samples were prepared as described (Oliveira *et al.*, 2016) and further separated by electrophoresis on 16% (w/v) SDS-polyacrylamide gels. After separation, LPS were detected by the Pro-Q™ Emerald 300 Lipopolysaccharide Gel Stain Kit (Life Technologies, Carlsbad, CA, USA), and visualized by UV-light radiation on a GelDoc™ XR+ system (Bio-Rad, Hercules, CA, USA). Quantitation of LPS was determined by densitometry analysis using the ImageJ software (Abràmoff *et al.*, 2004). In brief, images of stained gels were processed by quantifying pixel intensity values of all bands detected in a given lane as previously described (Peterson,

2010), and LPS amount was determined against a calibration curve established with *P. aeruginosa* LPS (Sigma-Aldrich, Burlington, MA, USA) as standard, whose samples were separated in the same gel.

Characterization of isolated Synechocystis extracellular vesicles

To characterize *Synechocystis* EVs, various methods were used to complement the SDS-PAGE analysis described above, namely by determining their amount and size (by nanoparticle tracking analysis, and TEM), and their morphological aspect (by TEM). Thus, EVs samples from *Synechocystis* wild type and mutant strains were analysed on a NanoSight NS300 (Malvern, Malvern, UK), equipped with an sCMOS camera. EVs samples were diluted in filtered PBS solution (between 1:1000 and 1:10 000), and further analysed as described (Oliveira *et al.*, 2016). In brief, five movies of 30 s were recorded for each sample (with a threshold of 10–50 particles per frame), with the following capturing settings: camera level 14, slider shutter 800–1300, slider gain 350–500, at 25°C and with a syringe pump speed of 40. Data acquisition and processing were performed using the NanoSight NS300 NTA 3.0 software (Malvern), using a detection threshold of 5.

Furthermore, for negative staining transmission electron microscopy, 10 µl of EVs preparations from the various cyanobacterial strains were mounted on formvar/carbon film coated mesh nickel grids (EMS, Hatfield, PA, USA) and left standing for 2 min. The liquid in excess was removed with filter paper, and 10 µl of 1% uranyl acetate was added on to the grids and left standing for 10 s, after which liquid in excess was removed with filter paper. Visualization was carried out on a Jeol JEM-1400 transmission electron microscope at 80 kV. Vesicle size was determined by direct measurement from electron micrographs using the open source software ImageJ (Abràmoff *et al.*, 2004). Several micrographs obtained from three biological replicates were used, and the diameter of more than 300 (WT), 450 ($\Delta toIC$), 550 ($\Delta toIC/\Delta spy$), 350 ($\Delta fucS$) and 370 (EV-trc-GFP) particles was measured.

For immunogold labelling of sfGFP-loaded EVs, vesicles were isolated as described above. EVs were fixed in 2% (w/v) paraformaldehyde and 0.05% (v/v) glutaraldehyde prepared in 0.1 M sodium cacodylate buffer for 2 h, and then washed twice in the same buffer, without the fixing agents (30 min per incubation step). Later, the EVs sample was dehydrated according to the following scheme: 15 min in 50% (v/v) ethanol; twice in 70% (v/v) ethanol (30 min each incubation); twice in 100% (v/v) ethanol (30 min each incubation). For resin infiltration, the EVs sample was treated for 1 h with a mix of LR

White resin and 100% (v/v) ethanol in a proportion of 2:1, twice for 1 h with LR White resin, once overnight in fresh LR White resin, and, finally, 1 h in fresh LR White resin. Resin polymerization was achieved by incubating samples at 60°C for 24 h. Sections were then washed in Tris-buffered saline solution (TBS: 50 mM of Tris-HCl, 150 mM of NaCl, pH 7.6) for 10 min, and incubated in 14.4% (w/v) sodium metaperiodate (antigen retrieval) for 1 h. Later, sections were washed in TBS for 10 min and in 20 mM of glycine for 5 min, and incubated with blocking solution (2% (w/v) BSA in TBS) for 30 min, before being incubated overnight, at 4°C, with a GFP specific monoclonal mouse antibody (Roche), diluted 1:100 in blocking solution supplemented with 3% (w/v) NaCl. Samples were washed three times in 0.1% (w/v) BSA in TBS (4 min each wash), blocked for 20 min in blocking solution and incubated with a goat anti-mouse IgG (H + L) conjugated with gold nanoparticles (15 nm) (BBI International) for 1 h. Then, samples were washed four times in TBS (2 min each), treated with 1% (w/v) glutaraldehyde in TBS for 5 min, washed again 6 times with distilled water (10 min each wash) and finally contrasted with uranyl acetate (5 min) and lead citrate (5 min). Visualization was carried out on a Jeol JEM-1400 transmission electron microscope at 80 kV.

Confocal microscopy analysis of Synechocystis cells

Synechocystis cells from the mutant strain EV-trc-GFP, and its derived EVs, were visualized on a Leica TCS SP5 II confocal microscope (Leica Microsystems, Wetzlar, Germany). EV-trc-GFP cells were cultivated in glass gas washing bottles as described above to an OD₇₃₀ of 1.5. Ten micro litres of cell suspension or 2 µl of EVs suspension were laid onto glass slides covered with solid BG11 medium supplemented with 1% low-melting agarose, and later visualized. GFP emission (collected between 500 and 540 nm) was observed when samples were exposed to a laser beam at 488 nm, while cyanobacterial cell autofluorescence was collected between 610 and 680 nm after excitation at 488 nm.

Protein extraction and analysis

To obtain total protein extracts, *Synechocystis* wild type or EV-trc-GFP cells were cultivated to an OD₇₃₀ of approximately 1.5, collected by centrifugation (4400 g, 10 min, at room temperature), suspended in protein extraction buffer (Lopes Pinto *et al.*, 2011) and sonicated as described (Gonçalves *et al.*, 2018). Cell debris was collected by centrifugation (10 000 g, 10 min, 4°C), and the cell free, total protein extract was stored at –20°C until further analysis. Total protein quantification was determined using the Bradford assay (BioRad). A total

volume of 600 ml of extracellular medium recovered after culture centrifugation was filtered through 0.45 µm pore size filters to remove any contaminating cells, and EVs were isolated as described above. Soluble extracellular proteins were recovered by concentrating the EV-free extracellular medium by ultrafiltration using centrifugal filters with a molecular weight cut-off of 3 kDa (Millipore). Concentrated samples were stored at -20°C until further analysis.

For protein analyses, samples were separated by standard electrophoresis on SDS-polyacrylamide gels, and gels were stained with Coomassie brilliant blue G (Sigma-Aldrich) for visualization of the peptide profile. For Western blotting, after electrophoretic separation, proteins were transferred from the gels to nitrocellulose membrane filters. Membranes were blocked for 3 h with 5% (w/v) milk powder in TBS-T [TBS with 0.05% (v/v) Tween 20] and then incubated overnight at 4°C with GFP-specific monoclonal mouse antibody (Roche, Basel, Switzerland) in fresh blocking buffer. After washing with TBS-T, blots were incubated for 1 h with goat anti-mouse IgG (Invitrogen, Waltham, MA, USA) linked to horseradish peroxidase. Membranes were washed with TBS-T before immunodetection, which was performed by chemiluminescence using ECL Western Blotting Analysis System detection reagents. Quantitation of relative band intensity was determined by densitometry analysis, using the ImageJ software as previously described (Peterson, 2010).

Ethics statement

Animal experiments were approved by the Animal Welfare and Ethics Body (ORBEA) committee of the Interdisciplinary Centre of Marine and Environmental Research (CIIMAR). This study was directed by accredited scientists (following FELASA category C recommendations) and all animal procedures were conducted in compliance with the guidelines provided by the International Guiding Principles for Research Involving Animals (EU 2010/63).

Zebrafish husbandry and breeding

Wild-type zebrafish (*Danio rerio*) were maintained in a recirculating water system under standard husbandry conditions (water temperature of $28 \pm 1^\circ\text{C}$; oxygen between $7.5\text{--}8\text{ mg l}^{-1}$; ammonia and nitrite levels kept around 0 mg l^{-1} ; and photoperiod of 14 h light/10 h dark). Fish were fed TetraMin tropical flakes (Tetra) twice a day. Adult fish were maintained at sex ratio of two males to one female, and group in-tank breeding was achieved with the addition of artificial nests to aquaria on the day prior to embryo collection. Embryos were collected 1 h after light onset, cleaned, separated from

unfertilized eggs and incubated in sterile Petri dishes with zebrafish embryo medium [egg water: 60 mg l^{-1} of Sea Salt (Instant Ocean, Blacksburg, VA, USA) in deionized water], at pH 7.2, containing 0.38 mg l^{-1} methylene blue (Sigma-Aldrich) at 28°C.

For confocal microscopy analyses, fish were fed with SPAROS thrice a day. Adult fish were maintained in breeding cages at sex ratio two females to one male on the night prior to embryo collection. Next morning, upon light onset, the divider was removed, and fish started to reproduce. Breeding tanks are equipped with a net at the bottom, so the eggs can fall through the net, avoiding to be eaten by adult fish. Eggs were collected, cleaned and incubated at 28°C in embryo medium (E3 – NaCl, KCl, $\text{CaCl}_2 \cdot 2\text{H}_2\text{O}$ and $\text{MgCl}_2 \cdot 6\text{H}_2\text{O}$), with 0.2 mM of 1-phenyl-2-thiourea to avoid pigmentation development.

Zebrafish challenge with *Synechocystis* LPS and EVs

The effects of LPS and EVs from *Synechocystis* wild-type and mutant strains *tolC*, *tolC/spy*, *fucS* on the survival of zebrafish larvae with 3 days post-fertilization were assessed by immersion trials performed in 6-well flat-bottom plates (Sarstedt, Nümbrecht, Germany) incubated at 28°C, in a final volume of 6 ml, for 5 days. The LPS or EVs of each *Synechocystis* strain were tested at 250 and 500 µg LPS ml⁻¹ in egg water, against a zebrafish embryo medium control treatment and a positive control treatment of 45 µg ml⁻¹ of commercial *Pseudomonas aeruginosa* LPS (Sigma) in zebrafish embryo medium. Treatments were tested in triplicates of 12 larvae, and each experiment was performed twice (two biological replicates), making a total of 72 larvae analysed within each experimental condition.

To assess how EVs from *Synechocystis* mutant strains *tolC* and *fucS* affect gene expression of inflammation associated markers, 3 dpf zebrafish larvae were subject to 250 and 500 µg LPS ml⁻¹ of EVs from each strain, against a zebrafish embryo medium control and 35 µg ml⁻¹ of commercial *P. aeruginosa* LPS (sub-lethal concentration) in zebrafish embryo medium, used as positive control. All treatments were tested six times, in 6-well flat-bottom plates, with 20 larvae and 10 ml of solution per well. At the end of the trials, larvae from each well were pooled and stored in RNeasy for gene expression analysis.

RNA extraction, cDNA synthesis and Gene expression analysis

Total RNA was extracted from 20 larvae pools, using the Direct-zol™ RNA MiniPrep Kit (Zymo Research, Irvine, CA, USA), according to manufacturer's

recommendations. Prior to extraction, larvae pools were homogenized with 1 ml of TRIzol reagent using 1.4 mm ceramic beads, and three cycles of 10 s at 7200 rpm in a Precellys Evolution homogenizer (Bertin Technologies, Montigny-le-Bretonneux, France). RNA was eluted in 50 μ l of DEPC-treated water, its integrity confirmed by agarose gel electrophoresis and its quality measured with a Multiskan GO Spectrophotometer equipped with a μ Drop™ Plate (Thermo Fisher Scientific, Waltham, MA, USA).

cDNA was generated from 1 μ g of total RNA using the NZY First-Strand cDNA Synthesis Kit (NZYTech, Lisbon, Portugal), and stored at -20°C until further analysis.

Real-time PCR was performed with a CFX Connect Real-Time PCR system (BioRad) using SsoAdvanced Universal SYBR Green Supermix (BioRad), according to the manufacturer's protocol. PCR reactions were set up using 0.5 μ l of 10 μ M of each primer (Table S8) and 0.5 μ l of 2-fold diluted cDNA in a reaction volume of 10 μ l. Reactions specificity was verified using melting curve analysis and absence of primer dimer. Standard curves were obtained for each cDNA template by plotting C_t values against the \log_{10} of six different dilutions of a cDNA mix solution from all samples analysed. Real-time PCR efficiency (E) was calculated from a standard curve according to the equation $E = 10(-1/\text{slope})$. Rpl13a was selected as the endogenous control gene (Table S8) and gene expression of the control group was used as calibrator.

Statistical analysis

Survival curves were plotted using the Kaplan–Meier method and pairwise comparisons between treatments were performed with nonparametric log-rank test, at 0.05 significance level, in GraphPad Prism version 9 (GraphPad Software Inc., San Diego, CA, USA). Gene expression data was checked for normal distribution and homogeneity of variances and normalized when appropriate. When found, extreme outliers, that is data values which lie more than three times the interquartile range below the first quartile or above the third quartile, were removed from the analysis. Treatments effects were analysed by one-way ANOVA and significant differences among means ($P < 0.05$) were determined by the Tukey's multiple range test, using SPSS for Windows version 26 software package (IBM SPSS Statistics, Armonk, NY, USA).

Confocal microscopy analysis of zebrafish larvae treated with sfGFP-loaded *Synechocystis* EVs

To study the possibility of carrying sfGFP to zebrafish via *Synechocystis* EVs, 5 dpf zebrafish larvae were

subjected to immersion trials performed in 24-well flat-bottom plates (Sarstedt) incubated at 28°C , in a final volume of 2 ml, for 24 h. Three zebrafish larvae were treated with 0 (control) or 1000 $\mu\text{g ml}^{-1}$ of sfGFP-loaded EVs in zebrafish embryo medium. Each experiment was performed three times. After the incubation period, zebrafish larvae were euthanized by subjecting the larvae to a lethal dose of 300 mg l^{-1} of tricaine methanesulfonate (MS222), immediately mounted on a glass slide, with 50% glycerol in PBS solution as mounting medium, and visualized by confocal microscopy (Leica TCS SP5 II). The sfGFP signal was collected between 495 and 540 nm upon exposing the specimens to a laser beam of 488 nm, using the same acquisition settings for all tested conditions. In addition, differential interference contrast (DIC) images were also acquired.

Acknowledgements

The authors acknowledge the support of the i3S Scientific Platforms 'Histology and Electron Microscopy' and 'Advanced Light Microscopy', members of the national infrastructure Portuguese Platform of Bioimaging (PPBI-POCI-01-0145-FEDER-022122). This work was financed by Fundo Europeu de Desenvolvimento Regional (FEDER) funds through the COMPETE 2020 Operational Programme for Competitiveness and Internationalisation (POCI), Portugal, 2020, and by Portuguese funds through Fundação para a Ciência e a Tecnologia/Ministério da Ciência, Tecnologia e Ensino Superior in the framework of the project POCI-01-0145-FEDER-029540 (PTDC/BIA-OUT/29540/2017), and PTDC/BIA-MOL/3834/2021. Fundação para a Ciência e a Tecnologia is also greatly acknowledged for the PhD fellowships SFRH/BD/130478/2017 (SL) and SFRH/BD/147762/2019 (AE), and individual supporting grants CEECIND/03482/2018 (JB) and IF/00256/2015 (PO).

Conflict of interest

None declared.

References

- Abed, R.M.M., Dobretsov, S., and Sudesh, K. (2009) Applications of cyanobacteria in biotechnology. *J Appl Microbiol* **106**: 1–12.
- Abramoff, M.D., Magalhães, P.J., and Ram, S.J. (2004) Image processing with ImageJ. *Biophoton Int* **11**: 36–42.
- Alves, N.J., Turner, K.B., Medintz, I.L., and Walper, S.A. (2016) Protecting enzymatic function through directed packaging into bacterial outer membrane vesicles. *Sci Rep* **6**: 24866.
- Badarau, A., Firbank, S.J., Waldron, K.J., Yanagisawa, S., Robinson, N.J., Banfield, M.J., and Dennison, C. (2008)

- FutA2 is a ferric binding protein from *Synechocystis* PCC 6803. *J Biol Chem* **283**: 12520–12527.
- Billar, S.J., Lundeen, R.A., Hmelo, L.R., Becker, K.W., Arellano, A.A., Dooley, K., *et al.* (2022a) *Prochlorococcus* extracellular vesicles: molecular composition and adsorption to diverse microbes. *Environ Microbiol* **24**: 420–435.
- Billar, S.J., Muñoz-Marín, M.D.C., Lima, S., Matinha-Cardoso, J., Tamagnini, P., and Oliveira, P. (2022b) Isolation and characterization of cyanobacterial extracellular vesicles. *J Vis Exp* **180**: e63481.
- Bonnington, K.E., and Kuehn, M.J. (2014) Protein selection and export via outer membrane vesicles. *Biochim Biophys Acta* **1843**: 1612–1619.
- Cai, Y.P., and Wolk, C.P. (1990) Use of a conditionally lethal gene in *Anabaena* sp. strain PCC 7120 to select for double recombinants and to entrap insertion sequences. *J Bacteriol* **172**: 3138–3145.
- Caruana, J.C., and Walper, S.A. (2020) Bacterial membrane vesicles as mediators of microbe – microbe and microbe – host community interactions. *Front Microbiol* **11**: 432.
- Dezfooli, S.M., Gutierrez-Maddox, N., Alfaro, A., and Seyfoddin, A. (2019) Encapsulation for delivering bioactives in aquaculture. *Rev Aquacult* **11**: 631–660.
- Durai, P., Batool, M., and Choi, S. (2015) Structure and effects of cyanobacterial lipopolysaccharides. *Mar Drugs* **13**: 4217–4230.
- Fantappiè, L., de Santis, M., Chiarot, E., Carboni, F., Bensi, G., Jousson, O., *et al.* (2014) Antibody-mediated immunity induced by engineered *Escherichia coli* OMs carrying heterologous antigens in their lumen. *J Extracell Vesicles* **3**: 24015.
- FAO (2020) *The State of World Fisheries and Aquaculture 2020. Sustainability in Action*. Rome, Italy: Food and Agriculture Organization of the United Nations.
- Ferreira, E.A., Pacheco, C.C., Pinto, F., Pereira, J., Lamosa, P., Oliveira, P., *et al.* (2018) Expanding the toolbox for *Synechocystis* sp. PCC 6803: validation of replicative vectors and characterization of a novel set of promoters. *Synth Biol* **3**: ysy014.
- Fisher, M.L., Allen, R., Luo, Y., and Curtiss, R. III (2013) Export of extracellular polysaccharides modulates adherence of the cyanobacterium *Synechocystis*. *PLoS One* **8**: e74514.
- Gonçalves, C.F., Pacheco, C.C., Tamagnini, P., and Oliveira, P. (2018) Identification of inner membrane translocase components of TolC-mediated secretion in the cyanobacterium *Synechocystis* sp. PCC 6803. *Environ Microbiol* **20**: 2354–2369.
- Hahn, A., and Schleiff, E. (2014) The cell envelope. In *The Cell Biology of Cyanobacteria*. Flores, E., and Herrero, A. (eds). Norfolk, UK: Caister Academic Press, pp. 29–87.
- Hai, N.V. (2015) The use of probiotics in aquaculture. *J Appl Microbiol* **119**: 917–935.
- Han, P., Lu, Q., Fan, L., and Zhou, W. (2019) A review on the use of microalgae for sustainable aquaculture. *Appl Sci* **9**: 2377.
- Heidorn, T., Camsund, D., Huang, H.-H., Lindberg, P., Oliveira, P., Stensjö, K., and Lindblad, P. (2011) Chapter twenty-four – Synthetic biology in cyanobacteria: engineering and analyzing novel functions. In *Methods in Enzymology*. Voigt, C. (ed). Cambridge, MA, USA: Academic Press, pp. 539–579.
- Hewelt-Belka, W., Kot-Wasik, Á., Tamagnini, P., and Oliveira, P. (2020) Untargeted lipidomics analysis of the cyanobacterium *Synechocystis* sp. PCC 6803: lipid composition variation in response to alternative cultivation setups and to gene deletion. *Int J Mol Sci* **21**: 8883.
- Jain, S., and Pillai, J. (2017) Bacterial membrane vesicles as novel nanosystems for drug delivery. *Int J Nanomed* **12**: 6329–6341.
- Kesty, N.C., and Kuehn, M.J. (2004) Incorporation of heterologous outer membrane and periplasmic proteins into *Escherichia coli* outer membrane vesicles. *J Biol Chem* **279**: 2069–2076.
- Kurban, K., Gao, X., Zhang, H., Liu, J., Dong, M., Wu, L., *et al.* (2020) Doxorubicin-loaded bacterial outer-membrane vesicles exert enhanced anti-tumor efficacy in non-small-cell lung cancer. *Acta Pharm Sin B* **10**: 1534–1548.
- Kwon, K.-C., Lamb, A., Fox, D., and Porphy Jegathese, S.J. (2019) An evaluation of microalgae as a recombinant protein oral delivery platform for fish using green fluorescent protein (GFP). *Fish Shellfish Immunol* **87**: 414–420.
- Lima, S., Matinha-Cardoso, J., Giner-Lamia, J., Couto, N., Pacheco, C.C., Florencio, F.J., *et al.* (2022) Extracellular vesicles as an alternative copper-secretion mechanism in bacteria. *J Hazard Mater* **431**: 128594. doi: 10.1016/j.jhazmat.2022.128594.
- Lima, S., Matinha-Cardoso, J., Tamagnini, P., and Oliveira, P. (2020) Extracellular vesicles: an overlooked secretion system in cyanobacteria. *Life (Basel)* **10**: 129.
- Lopes Pinto, F., Erasmie, S., Blikstad, C., Lindblad, P., and Oliveira, P. (2011) FtsZ degradation in the cyanobacterium *Anabaena* sp. strain PCC 7120. *J Plant Physiol* **168**: 1934–1942.
- Ma, K., Bao, Q., Wu, Y., Chen, S., Zhao, S., Wu, H., and Fan, J. (2020) Evaluation of microalgae as immunostimulants and recombinant vaccines for diseases prevention and control in aquaculture. *Front Bioeng Biotechnol* **8**: 590431.
- Morais Junior, W.G., Gorgich, M., Corrêa, P.S., Martins, A.A., Mata, T.M., and Caetano, N.S. (2020) Microalgae for biotechnological applications: cultivation, harvesting and biomass processing. *Aquaculture* **528**: 735562.
- Novoa, B., Bowman, T.V., Zon, L., and Figueras, A. (2009) LPS response and tolerance in the zebrafish (*Danio rerio*). *Fish Shellfish Immunol* **26**: 326–331.
- O'Donoghue, E.J., and Krachler, A.M. (2016) Mechanisms of outer membrane vesicle entry into host cells. *Cell Microbiol* **18**: 1508–1517.
- Oliveira, P., Martins, N.M., Santos, M., Pinto, F., Büttel, Z., Couto, N.A.S., *et al.* (2016) The versatile TolC-like Slr1270 in the cyanobacterium *Synechocystis* sp. PCC 6803. *Environ Microbiol* **18**: 486–502.
- Pandiyani, P., Balaraman, D., Thirunavukkarasu, R., George, E.G.J., Subaramaniyan, K., Manikkam, S., and Sadayappan, B. (2013) Probiotics in aquaculture. *Drug Invention Today* **5**: 55–59.
- Park, K.-S., Choi, K.-H., Kim, Y.-S., Hong, B.S., Kim, O.Y., Kim, J.H., *et al.* (2010) Outer membrane vesicles derived from *Escherichia coli* induce systemic inflammatory response syndrome. *PLoS One* **5**: e11334.

- Park, M., Sun, Q., Liu, F., DeLisa, M.P., and Chen, W. (2014) Positional assembly of enzymes on bacterial outer membrane vesicles for cascade reactions. *PLoS One* **9**: e97103.
- Peterson, T. (2010) Densitometric analysis using NIH image. *North American Vascular Biology Organization (NAVBO) eNewsletter* **16**.
- Pinto, F., Pacheco, C.C., Oliveira, P., Montagud, A., Landels, A., Couto, N., *et al.* (2015) Improving a *Synechocystis*-based photoautotrophic chassis through systematic genome mapping and validation of neutral sites. *DNA Res* **22**: 425–437.
- Pitt, J.A., Kozal, J.S., Jayasundara, N., Massarsky, A., Trevisan, R., Geitner, N., *et al.* (2018) Uptake, tissue distribution, and toxicity of polystyrene nanoparticles in developing zebrafish (*Danio rerio*). *Aquat Toxicol* **194**: 185–194. doi: 10.1016/j.aquatox.2017.11.017.
- Polyviou, D., Machelett, M.M., Hitchcock, A., Baylay, A.J., MacMillan, F., Moore, C.M., *et al.* (2018) Structural and functional characterization of IdiA/FutA (Tery_3377), an iron-binding protein from the ocean diazotroph *Trichodesmium erythraeum*. *J Biol Chem* **293**: 18099–18109.
- van Pomeran, M., Brun, N.R., Peijnenburg, W.J.G.M., and Vijver, M.G. (2017) Exploring uptake and biodistribution of polystyrene (nano) particles in zebrafish embryos at different developmental stages. *Aquat Toxicol* **190**: 40–45. doi: 10.1016/j.aquatox.2017.06.017.
- Quan, S., Koldewey, P., Tapley, T., Kirsch, N., Ruane, K.M., Pfizenmaier, J., *et al.* (2011) Genetic selection designed to stabilize proteins uncovers a chaperone called Spy. *Nat Struct Mol Biol* **18**: 262–269.
- Rezania, S., Amirmozaffari, N., Tabarraei, B., Jeddi-Tehrani, M., Zarei, O., Alizadeh, R., *et al.* (2011) Extraction, Purification and Characterization of Lipopolysaccharide from *Escherichia coli* and *Salmonella typhi*. *Avicenna J Med Biotechnol* **3**: 3–9.
- Rippka, R., Deruelles, J., Waterbury, J.B., Herdman, M., and Stanier, R.Y. (1979) Generic assignments, strain histories and properties of pure cultures of cyanobacteria. *J Gen Microbiol* **111**: 1–61.
- Schwechheimer, C., Kulp, A., and Kuehn, M.J. (2014) Modulation of bacterial outer membrane vesicle production by envelope structure and content. *BMC Microbiol* **14**: 324.
- Stewart, I., Schluter, P.J., and Shaw, G.R. (2006) Cyanobacterial lipopolysaccharides and human health – a review. *Environ Health* **5**: 7.
- Sendra, M., Pereira, P., Yeste, M., Mercado, L., Figueras, A., and Novoa, B. (2021) Size matters: Zebrafish (*Danio rerio*) as a model to study toxicity of nanoplastics from cells to the whole organism. *Environ Pollut* **268(Part A)**: 115769. doi: 10.1016/j.envpol.2020.115769.
- Swanson-Mungerson, M., Incrocci, R., Subramaniam, V., Williams, P., Hall, M.L., and Mayer, A.M.S. (2017) Effects of cyanobacteria *Oscillatoria* sp. lipopolysaccharide on B cell activation and Toll-like receptor 4 signaling. *Toxicol Lett* **275**: 101–107.
- Waldron, K.J., Tottey, S., Yanagisawa, S., Dennison, C., and Robinson, N.J. (2007) A periplasmic iron-binding protein contributes toward inward copper supply. *J Biol Chem* **282**: 3837–3846.
- Yao, Y.-Y., Yang, Y.-L., Gao, C.-C., Zhang, F.-L., Xia, R., Li, D., *et al.* (2020) Surface display system for probiotics and its application in aquaculture. *Rev Aquacult* **12**: 2333–2350.
- Yin, H., Chen, C.Y., Liu, Y.W., Tan, Y.J., Deng, Z.L., Yang, F., *et al.* (2019) *Synechococcus elongatus* PCC7942 secretes extracellular vesicles to accelerate cutaneous wound healing by promoting angiogenesis. *Theranostics* **9**: 2678–2693.
- Zavan, L., Bitto, N.J., and Kaparakis-Liaskos, M. (2020) Introduction, history, and discovery of bacterial membrane vesicles. In *Bacterial Membrane Vesicles*. Kaparakis-Liaskos, M., and Kufer, T. (eds). Cham, Switzerland: Springer, pp. 1–21.

Supporting information

Additional supporting information may be found online in the Supporting Information section at the end of the article.

Table S1. Survival percentages of 3 days post-fertilization (dpf) zebrafish larvae subjected to zebrafish embryo medium containing 250 or 500 $\mu\text{g mL}^{-1}$ of LPS or EVs from *Synechocystis* sp. PCC 6803 wild-type (WT), and mutant strains ΔtolC , $\Delta\text{tolC}/\Delta\text{spy}$ and ΔfucS . Survival was monitored for 5 days (120 h) of immersion challenge. Control treatments received zebrafish embryo medium only (CTR) or zebrafish embryo medium containing commercial LPS from *Pseudomonas aeruginosa* (LPS Pa) at 45 $\mu\text{g mL}^{-1}$.

Table S2. *P*-values for pairwise comparisons with the log-rank test between the survival curves of zebrafish larvae subjected to *Synechocystis* sp. PCC 6803 wild-type extracellular vesicles (EVs WT), LPS, and *Pseudomonas aeruginosa* LPS (LPS Pa), at the indicated concentrations ($\mu\text{g mL}^{-1}$). Control refers to larvae exposed to Egg water only.

Table S3. *P*-values for pairwise comparisons with the log-rank test between the survival curves of zebrafish larvae subjected to *Synechocystis* sp. PCC 6803 ΔtolC mutant extracellular vesicles (EVs), LPS, and *Pseudomonas aeruginosa* LPS (LPS Pa), at the indicated concentrations ($\mu\text{g mL}^{-1}$). Control refers to larvae exposed to Egg water only.

Table S4. *P*-values for pairwise comparisons with the log-rank test between the survival curves of zebrafish larvae subjected to *Synechocystis* sp. PCC 6803 $\Delta\text{tolC}/\Delta\text{spy}$ mutant extracellular vesicles (EVs), LPS, and *Pseudomonas aeruginosa* LPS (LPS Pa), at the indicated concentrations ($\mu\text{g mL}^{-1}$). Control refers to larvae exposed to Egg water only.

Table S5. *P*-values for pairwise comparisons with the log-rank test between the survival curves of zebrafish larvae subjected to *Synechocystis* sp. PCC 6803 ΔfucS mutant extracellular vesicles (EVs), LPS, and *Pseudomonas aeruginosa* LPS (LPS Pa), at the indicated concentrations ($\mu\text{g mL}^{-1}$). Control refers to larvae exposed to Egg water only.

Table S6. Results of *post hoc* Tukey's tests after one-way ANOVA of quantitative gene expression of the genes encoding Interleukin 1 beta (IL-1 β), Tumor necrosis factor alpha (TNF- α), and Interleukin 10 (IL-10) in zebrafish larvae immersed in zebrafish embryo medium only (CTR – control), zebrafish embryo medium containing 250 or 500 μg LPS mL^{-1} of EVs from *Synechocystis* mutants ΔtolC (EVs ΔtolC)

and $\Delta fucS$ (EVs $\Delta fucS$), or in zebrafish embryo medium containing 35 $\mu\text{g LPS mL}^{-1}$ of *P. aeruginosa* (LPS *Pa*). Data obtained from $n=6$, with each replicate representing a pool of 20 larvae. Statistical differences in gene expression by ANOVA ($p < 0.05$) are represented in bold.

Table S7. List of *Synechocystis* sp. PCC 6803 strains used in this work.

Table S8. Oligonucleotide primers used in this study.

Fig. S1. Generation of the *Synechocystis* sp. PCC 6803 *fucS*- and *tolC*-*spy*-mutant strains. Green-safe stained agarose gels showing the result of a PCR testing the extent of chromosome segregation of *Synechocystis* cells in which the genes *fucS* (left-hand side) or *spy* (right-hand side) were partially deleted in the wild-type or *tolC*-mutant backgrounds, respectively. $\Delta fucS$: lanes 1 and 2 correspond to two different clones; Δspy : lanes 1 and 2 correspond to two different clones. Genomic DNA from the *Synechocystis* wild-type (gWT) or *tolC*-mutant (g*tolC*) strains was used as the PCR positive control, while a reaction in which the DNA template was replaced by water (C⁻) was used as negative control. M, O'GeneRuler DNA ladder mix (Thermo Fisher Scientific). Selected sizes of the marker, and the exact size of the bands resulting from PCR amplification are shown in base pairs (bp).

Fig. S2. The *Synechocystis* sp. PCC 6803 strains used in this strain show different vesiculation capacities. The *Synechocystis* wild-type (WT), and the *tolC*- ($\Delta tolC$), *tolC*-*spy*- ($\Delta tolC \Delta spy$) and *fucS*- ($\Delta fucS$) mutant strains were cultivated under standard conditions and their vesicles isolated. Prior to loading, EVs samples were normalized for cell culture density (OD_{730}), volume of cell-free culture medium concentrated and concentration factor. EVs samples were then separated by electrophoresis on 16% (w/v) SDS-polyacrylamide gels, and stained with the Pro-QTM

Emerald 300 Lipopolysaccharide Gel Stain Kit (Life Technologies) for the detection of LPS as an outer membrane marker. The gel is representative of 3 independent biological replicates, and the densitometry analysis and quantification resulted in the graph presented in Figure 3A. On the left-hand side, schematic representation of the smooth-LPS (lipid A, oligosaccharide core, and O-antigen), and rough-LPS (lipid A and oligosaccharide core) that are found in *Synechocystis*.

Fig. S3. Characterization of the vesicles released by the *Synechocystis* sp. PCC 6803 strain EV-trc-GFP. A, Transmission electron micrograph representative of the morphological aspect of the vesicles released by EV-trc-GFP strain. Scale bar: 200 nm. B, The *Synechocystis* wild-type (WT) and EV-trc-GFP strains were cultivated under standard conditions and their EVs isolated. Prior to loading, samples were normalized for cell culture density (OD_{730}), volume of cell-free culture medium concentrated and concentration factor. EVs samples were then separated by electrophoresis on 16% (w/v) SDS-polyacrylamide gels, and stained with the Pro-QTM Emerald 300 Lipopolysaccharide Gel Stain Kit (Life Technologies) for the detection of LPS. The gel is representative of 5 independent biological replicates, and the densitometry analysis and quantification is shown on to the right. ***, $p < 0.001$. C, Histogram showing particle size distribution of EVs samples from the EV-trc-GFP strain. EVs were separated in 5 nm size groups, distributed between 30 and 130 nm, and in groups comprising those with a size below 30 nm or higher than 130 nm. Vesicle diameter was determined by direct measurement from electron micrographs of three independent biological replicates. Abundance of each size group is presented as relative figures, i.e. number of vesicles with a given diameter range relative to the total number of vesicles measured.